Bioorganic & Medicinal Chemistry 19 (2011) 3787–3792

Contents lists available at ScienceDirect

Bioorganic & Medicinal Chemistry

journal homepage: www.elsevier.com/locate/bmc

Self-assembly pathways of E22Δ-type amyloid β peptide mutants generated from non-aggregative *O*-acyl isopeptide precursors

Youhei Sohma [a,*,†], Hui Wang [a,†], Atsuhiko Taniguchi [a], Yuta Hirayama [a], Taeko Kakizawa [a], Moe Yamasaki [a], Hidehito Mukai [a,b], Yoshiaki Kiso [a,b,*]

[a] *Department of Medicinal Chemistry, Center for Frontier Research in Medicinal Science, Kyoto Pharmaceutical University, Yamashina-ku, Kyoto 607-8412, Japan*
[b] *Laboratory of Peptide Science, Nagahama Institute of Bio-Science and Technology, Nagahama, Shiga 526-0829, Japan*

ARTICLE INFO

Article history:
Received 13 April 2011
Revised 28 April 2011
Accepted 29 April 2011
Available online 6 May 2011

Keywords:
Aggregation
Amyloid
Alzheimer
Click peptide
Isopeptide
Mutant

ABSTRACT

The recently identified E22Δ-type amyloid β peptide (Aβ) mutants are reported to favor oligomerization over fibrillization and to exhibit more-potent synaptotoxicity than does wild-type (WT) Aβ. Aβ(E22Δ) mutants can thus be expected to serve as tools for clarifying the impact of Aβ oligomers in Alzheimer's disease (or Alzheimer's-type dementia). However, the biochemical and biophysical properties of Aβ(E22Δ) have not been conclusively determined. Here, we evaluated the self-assembly pathways of Aβ(E22Δ) mutants generated from water-soluble, non-aggregative *O*-acyl isopeptide precursors. Circular dichroism spectroscopy, Western blot analysis, and thioflavin-T fluorescence intensity and cellular toxicity assays suggest that the self-assembly pathways of Aβ(E22Δ) differed from those of Aβ(WT). Aβ1–40(E22Δ) underwent a rapid random coil→β-sheet conformational change in its monomeric or low-molecular-weight oligomeric states, whereas Aβ1–40(WT) self-assembled gradually without losing its propensity to form random coil structures. The Aβ1–42(E22Δ) monomer formed β-sheet-rich oligomers more rapidly than did Aβ1–42(WT). Additionally, the Aβ1–42(E22Δ) oligomers appear to differ from Aβ1–42(WT) oligomers in size, shape, or both. These results should provide new insights into the functions of Aβ(E22Δ) mutants.

1. Introduction

Alzheimer's disease (AD) is a severe neurodegenerative disease confined mostly to elderly populations. Cerebral accumulation of amyloid β peptides (Aβs) is widely believed to be the primary influence driving AD.[1] Aβs are a group of 38–43-residue proteolytic fragments released from amyloid precursor protein through sequential cleavages by β- and γ-secretases. Although Aβ1–40 is the predominant product of this proteolytic pathway, Aβ1–42 is far more fibrillogenic. Many missense mutations in the Aβ-coding region—mutations that are associated with familial early-onset AD—have also been identified, including Flemish (A21G), Arctic (E22G), Dutch (E22Q), Italian (E22K), Iowa (D23N), Japanese-Tottori (D7N), and English (H6R) mutations, each named after the region where it is prevalent.

One major obstacle to elucidation of the mechanisms of Aβ toxicity is their strong, uncontrollable tendency to self-assemble during experiments.[2] Various pretreatment methods have been used to select only monomeric Aβs for experiments, and the differing outcomes of Aβ studies may arise from differences in pretreatments. For example, the presence of residual disaggregating solvents (such as hexafluoroisopropanol) used for pretreatment may affect experiments. Moreover, monomeric Aβ1–42 starts to self-assemble during storage and handling prior to use. The self-assembly of Aβs leads to irreproducible and discrepant results.

We and others have used a 'click peptide' (also called 'switch-peptide') methodology by which monomeric Aβs can be predominantly obtained in situ from their *O*-acyl isopeptide derivatives (Fig. 1).[3–14] The presence of an *O*-acyl instead of *N*-acyl linkage at a hydroxyamino acid residue in the peptide backbone generally results in species with physicochemical properties different from those of the native peptide.[15–24] The *O*-acyl isopeptide of

Abbreviations: Aβ, amyloid β peptide; AD, Alzheimer's disease; CD, circular dichroism; DIC, *N*,*N*′-diisopropylcarbodiimide; DMAP, *N*,*N*-dimethyl-4-aminopyridine; DMEM, Dulbecco's modified Eagle's medium; DMF, *N*,*N*-dimethylformamide; DMSO, dimethyl sulfoxide; FBS, fetal bovine serum; HFIP, 1,1,1,3,3,3-hexafluoro-2-propanol; HOBt, *N*-hydroxybenzotriazole; HPLC, high-performance liquid chromatography; kDa, kilo-dalton of mass; MALDI, matrix assisted laser desorption ionization; MS, mass spectrometry; NGF, nerve growth factor; TFA, trifluroacetic acid; ThT, thioflavin-T; TOF, time of flight; UV, ultra-violet; WST-8, (2-(2-methoxy-4-nitrophenyl)-3-(4-nitrophenyl)-5-(24-disulfophenyl)-2*H*-tetrazolium. Amino acids are designated by standard one- and three-letter codes.

* Corresponding authors. Tel.: +81 75 595 4636; fax: +81 75 595 4787 (Y.S.); tel.: +81 749 64 8113; fax: +81 749 64 8140 (Y.K.).
E-mail addresses: ysohma@mb.kyoto-phu.ac.jp (Y. Sohma), y_kiso@nagahama-i-bio.ac.jp (Y. Kiso).
† These authors contributed equally.

0968-0896/$ - see front matter © 2011 Elsevier Ltd. All rights reserved.
doi:10.1016/j.bmc.2011.04.056

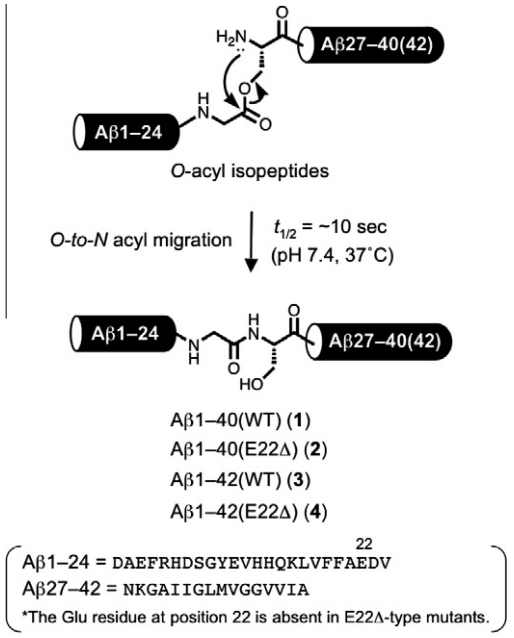

Figure 1. 'Click peptide' methodology. In situ production of Aβ1–40(WT) (**1**), Aβ1–40(E22Δ) (**2**), Aβ1–42(WT) (**3**), and Aβ1–42(E22Δ) (**4**) generated from the corresponding *O*-acyl isopeptides via an *O*-to-*N* intramolecular acyl migration reaction. The *O*-acyl isopeptides served as water-soluble and non-aggregative precursors to their respective native forms.

Aβ1–42, which has an ester bond between Gly[25] and Ser[26], has the following characteristics: (1) it is 100 times as water-soluble as Aβ1–42, owing to the protonated amino group at the isopeptide residue; (2) the monomer adopts a random coil structure (without forming amyloid fibrils) under acidic conditions, owing to the *O*-acyl isopeptide structure; and (3) changing the pH from acidic to neutral results in quick conversion to Aβ1–42 ($t_{1/2}$ ~10 s) via an *O*-to-*N* intramolecular acyl migration reaction (the 'click') with no by-product formation. As a result of this quick conversion, monomeric Aβ1–42 with a random coil structure can be predominantly produced in situ.

Recently, a E22Δ-type Aβ mutation, in which Glu[22] is missing, was identified from Japanese pedigrees displaying Alzheimer's-type dementia.[25] Aβ(E22Δ), which is the first amino acid deletion-type mutation to be discovered, reportedly favors oligomerization over fibrillization and exhibits more-potent synaptotoxicity than wild-type (WT) Aβ.[25–27] An enormous amount of work suggests that soluble Aβ(WT) oligomers, rather than monomers or insoluble amyloid fibrils, cause synaptic dysfunction.[28] However, the 'oligomer hypothesis' remains controversial, and unanswered questions remain. Which assemblies and structures of the oligomers (ranging from dimers to larger oligomers) are the toxic species? Do the Aβ oligomers by themselves cause synaptotoxicity without co-factors? Aβ(E22Δ) can be expected to serve as an experimental tool for investigating the mechanisms of Aβ oligomer action, and thus studying Aβ(E22Δ) is of broad biophysical and biochemical interest for expediting research on the assembly states of Aβs and the origins of their toxicity.

In addition to favoring oligomerization over fibrillization, Aβ(E22Δ) is also reported to promote β-sheet formation and radical production.[29] However, Meredith and co-workers reported that the Aβ1–40(E22Δ) forms fibrils instantaneously.[30] Thus, the biochemical and biophysical properties of Aβ(E22Δ) have not been conclusively determined. Here, we evaluated the properties of Aβ(E22Δ) mutants generated from non-aggregative *O*-acyl isopeptide precursors (Fig. 1). Circular dichroism (CD) spectroscopy, Western blot analysis, thioflavin-T (ThT) fluorescence intensity, and cellular toxicity assays suggest that the Aβ(E22Δ) mutants self-assembled by different mechanisms than does Aβ(WT).

2. Results and discussion

2.1. Secondary structure transitions verified by CD spectroscopy

O-Acyl isopeptides of Aβ1–40(WT) and Aβ1–40(E22Δ), synthesized using solid phase peptide synthesis, adopted random coil structures under acidic conditions (0.1% aqueous TFA solution) and underwent almost no conformational changes during incubation under acidic conditions for 24 h at 37 °C (Fig. S1). The results were in agreement with the results for *O*-acyl isopeptides of Aβ1–42(WT)[6] and Aβ1–42(E22Δ).[7]

To monitor the secondary structure transitions of Aβ1–40(WT) (**1**), Aβ1–40(E22Δ) (**2**), Aβ1–42(WT) (**3**), and Aβ1–42(E22Δ) (**4**), we neutralized stock solutions of the corresponding *O*-acyl isopeptides in 0.1% aqueous TFA solution by dilution with phosphate buffer (pH 7.4), and the neutralized solutions were incubated at 37 °C (final Aβ concentration, 10 μM). Under the neutral conditions, the *O*-acyl isopeptides were converted predominantly to the corresponding Aβs (**1**–**4**) within several minutes (Fig. S2 and Refs. 6 and 7). After incubation for 2 min, **1** displayed a CD spectrum characteristic of a random coil structure, and the structure remained nearly unchanged after 10 h of incubation (Fig. 2A). In contrast, **2** showed a CD spectrum characteristic of a β-structure right after neutralization of the peptide solution (right after the 'click', Fig. 2B), whereas its *O*-acyl isopeptide adopted a random coil structure under acidic conditions (Fig. S1B). This result suggests that **2** underwent a rapid random coil→β-sheet transition.[31] The amplitudes of the positive maximum at 200 nm and the negative maximum at 218 nm (characteristic of the β-sheet structure) increased over time (Fig. 2B).

For Aβ1–42(WT) (**3**), a gradual conversion from random coil to β-sheet structure was observed (Fig. 2C). For Aβ1–42(E22Δ) (**4**), the random coil spectrum observed after 2 min of incubation changed to a β-sheet spectrum within 30 min (Fig. 2D). These results suggest that the random coil-to-β-sheet transition of **4** was faster than that of **3**.

2.2. Oligomer formation verified by Western blot analysis

To verify the assembly states of the peptides, we incubated **1**–**4** (peptide concentration, 10 μM) generated from the corresponding *O*-acyl isopeptides in pH 7.4 phosphate buffer at 37 °C and then analyzed the solutions by Western blotting at various intervals. The size distributions were determined by SDS–PAGE on NuPAGE Bis–Tris 4–12% gel with 6E10 monoclonal antibody detection (Fig. 3 and S3). For Aβ1–40(WT) (**1**) and Aβ1–40(E22Δ) (**2**), bands corresponding to the molecular masses of the monomers were the only detected bands after incubation for 2 min (Figs. S3A and 3A, respectively). This result suggests that **1** and **2** were monomeric immediately after generation from the *O*-acyl isopeptides. For **1**, bands corresponding to monomer through trimer were observed during incubation for 7 days (Fig. S3A). Aβ1–40(E22Δ) (**2**) displayed a smear band corresponding to dimer over time (Fig. 3A). Because Aβ aggregates are affected by SDS (association, dissociation, or both occur in the presence of SDS),[32] the use of SDS–PAGE showed only SDS-stable Aβ oligomers. Nevertheless, the appearance of the bands, corresponding to the molecular masses of dimers and trimers, with incubation time might reflect the time-dependent self-assembly of **1** and **2**.

In the Western blot analysis of Aβ1–42(E22Δ) (**4**), a broad smear corresponding to a molecular mass exceeding 260 kDa was

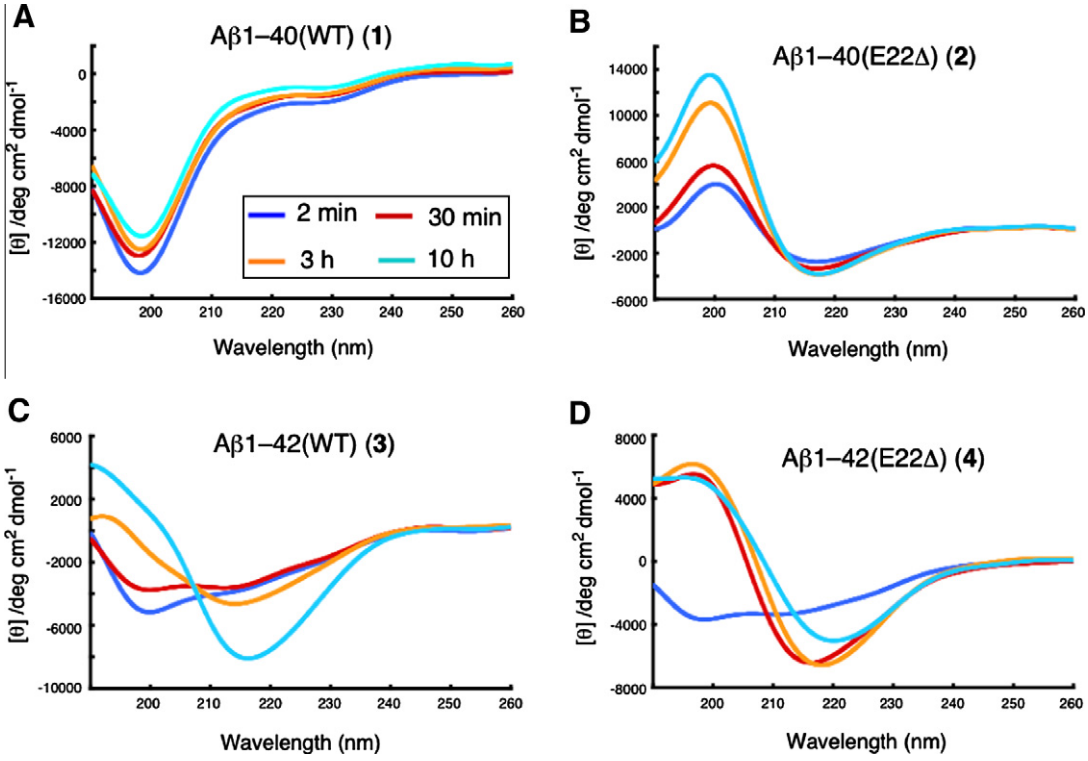

Figure 2. Secondary structure formation. (A) Aβ1–40(WT) (**1**), (B) Aβ1–40(E22Δ) (**2**), (C) Aβ1–42(WT) (**3**), and (D) Aβ1–42(E22Δ) (**4**) generated from the corresponding *O*-acyl isopeptides were incubated at concentrations of 10 μM in pH 7.4 phosphate buffer at 37 °C, and the solutions were analyzed by CD.

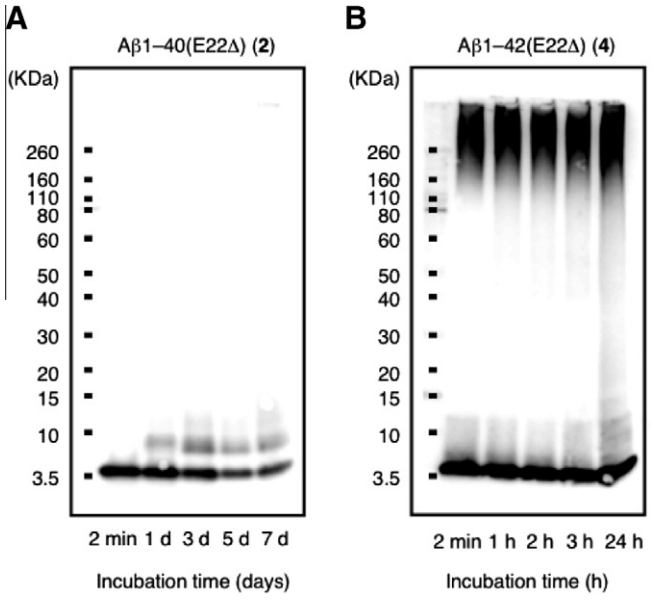

Figure 3. Western blot analysis of (A) Aβ1–40(E22Δ) (**2**) and (B) Aβ1–42(E22Δ) (**4**). The species were separated by SDS–PAGE on a 4–12% NuPAGE Bis–Tris gel with monoclonal antibody 6E10 detection (the epitope lies within amino acid residues 3–8). Note that Aβ(E22Δ) was not stained well with 4G8 (the epitope lies within amino acid residues 18–22). Aβ1–40(E22Δ) (**2**) and Aβ1–42(E22Δ) (**4**) generated from the corresponding *O*-acyl isopeptides were incubated at concentrations of 10 μM in pH 7.4 phosphate buffer at 37 °C and then analyzed.

detected as soon as the peptide solution was neutralized (Fig. 3B), and intensity of the band did not change much during a 24-h incubation period. In contrast, in the analysis of Aβ1–42(WT) (**3**), bands at around 50–160 kDa and at the top of the gel were detected as the incubation time increased, and the intensity of these bands increased at the expense of the band for the monomer (Fig. S3B). Aβ1–42(WT) (**3**) and Aβ1–42(E22Δ) (**4**) showed similar tendencies toward oligomer formation when 82E1 antibody was used as the probe (Fig. S4). These results are in agreement with previously reported results indicating that Aβ1–42(E22Δ) forms oligomers immediately after solubilization and that the quantities of oligomers do not decline markedly, suggesting that Aβ1–42(E22Δ) favors the oligomer states more than does the WT.[25] Note that in our SDS–PAGE system, the size distribution of the oligomer bands for **4** differed from that for **3** in that no 50–160 kDa bands were observed for the former. This result suggests that Aβ1–42(E22Δ) formed oligomers with sizes or shapes distinct from those of the oligomers formed by Aβ1–42(WT).

2.3. Aggregation properties verified by ThT fluorescence intensity assay

ThT fluorescence intensity generally corresponds to the extent of β-sheet-rich Aβ aggregation. Mori and co-workers reported that the Aβ1–40(E22Δ) and Aβ1–42(E22Δ) exhibit remarkably lower ThT fluorescence intensities than the corresponding WT Aβs, and these results led them to hypothesize that E22Δ-type Aβs have low or no tendency to fibrillize.[25] However, inconsistent ThT assay results have been reported: Irie and co-workers reported that the fluorescence intensities of Aβ1–40(E22Δ) and Aβ1–42(E22Δ) increased over time, at a rate similar to that for Aβ1–42(WT), whereas Aβ1–40(WT) showed no significant increase in intensity.[29]

The ThT fluorescence intensities of **1**–**4** generated from the corresponding *O*-acyl isopeptides increased to varying degrees over a 48-h incubation period (Fig. 4A). The fluorescence profile of Aβ1–40(E22Δ) (**2**) was similar to that of Aβ1–40(WT) (**1**). The fluorescence intensities of Aβ1–42(E22Δ) (**4**) and Aβ1–42(WT) (**3**) initially increased at a similar rate, but the increase rate for **4**

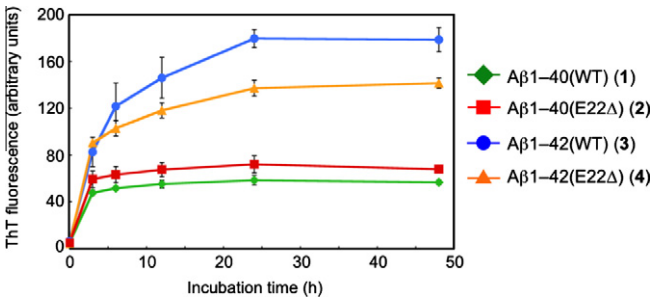

Figure 4. ThT assay. Aβ1–40(WT) (**1**), Aβ1–40(E22Δ) (**2**), Aβ1–42(WT) (**3**), and Aβ1–42(E22Δ) (**4**) generated from the corresponding *O*-acyl isopeptides were incubated at concentrations of 10 μM in pH 7.4 phosphate buffer at 37 °C and then their ThT fluorescence intensity was assayed. Values are means ± SEM for six experiments.

eventually slowed relatively to that of **3**. These results suggest that there was little difference in ThT fluorescence intensity (which often corresponds to the extent of aggregation) between Aβ(E22Δ) and Aβ(WT) obtained by means of the click peptide methodology, although we could not distinguish between oligomers and fibrils under the ThT assay conditions.

2.4. Cytotoxicity to PC12 cells

We determined the cytotoxicity of Aβ1–40(E22Δ) (**2**) and Aβ1–42(E22Δ) (**4**) generated from the corresponding *O*-acyl isopeptides. NGF-differentiated rat pheochromocytoma PC12 cells[33] in HEPES-DMEM containing 1% horse serum (final pH 7.4, under 10% CO_2) was used as a model system to test for cell toxicity induced by Aβs. The cells were incubated for 48 h in the presence of **1**–**4** (20 μM each) at 37 °C, and then cell viabilities were determined from the absorbance of soluble formazan dye formed from WST-8 reagent (Fig. 5). Aβ1–42(E22Δ) (**4**) exhibited no significant cytotoxicity to NGF-differentiated PC12 cells at 20 μM, at which concentration cell viability was reduced by 60% in the presence of Aβ1–42(WT) (**3**). Both **1** and **2** showed low cytotoxicity. Similar results were obtained with non-differentiated PC12 cells; **3** dramatically reduced cell viability (by approximately 90%), whereas **1**, **2**, and **4** showed no significant cytotoxicity (Fig. S5). These results are consistent with reports that Aβ1–42(E22Δ) has potent synaptotoxicity but no significant cytotoxicity for mouse neuroblastoma Neuro-2a and human neuroblastoma IMR-32 cells.[26] Interestingly, Flemish (A21G), Arctic (E22G), Dutch (E22Q), Italian (E22 K), Iowa (D23 N), Japanese-Tottori (D7 N), and English (H6R) Aβ1–42 mutants reportedly show similar or higher cytotoxicity in PC12 cells as compared to Aβ1–42(WT),[33,34] suggesting that Aβ1–42(E22Δ) acts by a synaptotoxicity[25] mechanism distinct from that of the WT and other mutants.

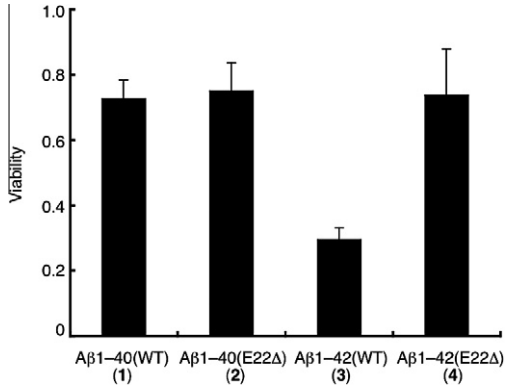

Figure 5. Cytotoxicity to NGF-differentiated PC12 cells. Aβ1–40(WT) (**1**), Aβ1–40(E22Δ) (**2**), Aβ1–42(WT) (**3**), and Aβ1–42(E22Δ) (**4**) generated from the corresponding *O*-acyl isopeptides were incubated at concentrations of 20 μM and 37 °C for 48 h and then analyzed. Values are means ± SEM from three independent experiments. Viability = [absorbance of soluble formazan dye formed from WST-8 in the presence of **1**–**4**]/[absorbance of soluble formazan dye formed from WST-8 in the absence of Aβ species (negative control)].

3. Conclusion

Our results suggest that the self-assembly mechanism of Aβ(E22Δ) mutants differed from that of WT Aβs. CD spectroscopy and Western blot analysis (Figs. 2B and 3A) indicate that Aβ1–40(E22Δ) (**2**) underwent a rapid random coil→β-sheet conformational change in its monomeric or low-molecular-weight oligomer states. In contrast, Aβ1–40(WT) (**1**) self-assembled without losing its propensity to form random coil structures (Fig. 2A and S3A). The tendency of Aβ1–40(E22Δ) (**2**) to form β-sheets was exceptional; such β-sheet-forming structures have been mostly observed for large oligomers and fibril states of Aβ. Aβ1–40(E22Δ) generated from amyloid precursor protein by means of enzymatic processing may undergo a similar conformational change involving rapid β-sheet formation. The monomer of Aβ1–42(E22Δ) (**4**) self-assembled to oligomers with β-sheet-rich structures more rapidly than did Aβ1–42(WT) (**3**), as indicated by CD spectroscopy and Western blot analysis. The differences between the size distributions of the oligomer bands for **3** and **4** suggest that the oligomers formed by Aβ1–42(E22Δ) differed in size, shape, or both from oligomers formed by Aβ1–42(WT). That the oligomer bands of **4** persisted throughout the incubation period supports the hypothesis that Aβ1–42(E22Δ) favored oligomeric states. The ThT fluorescence intensity profile of **4** was almost comparable to that of **3**. Moreover, the cytotoxicity of **4** to NGF-differentiated PC12 cells was remarkably lower than that of **3**. We believe that our results will provide new insights into the self-assembly mechanisms of the E22Δ-type Aβ mutants.

4. Experimental

4.1. General

All protected amino acids and resins were purchased from Calbiochem-Novabiochem Japan Ltd (Tokyo, Japan). HEPES buffered Dulbecco's modified Eagle's medium (DMEM), fetal bovine serum (FBS) and horse serum were purchased from Invitrogen (Carlsbad, CA), MP Biomedicals, Inc. (Irvine, CA) and SAFC Biosciences (Lenexa, KS), respectively. Rat pheochromocytoma PC12 cells were obtained from Riken BioResource Center (Ibaraki, Japan). Other chemicals were purchased from commercial suppliers, Wako Pure Chemical Ind., Ltd (Osaka, Japan), Nacalai Tesque (Kyoto, Japan), Kanto Chemical Co., Inc. (Tokyo, Japan), Watanabe Chemical Ind., Ltd (Hiroshima, Japan), Dojin Laboratories (Kumamoto, Japan) and Sigma–Aldrich, Inc. (Milwaukee, WI, USA) and were used without further purification. MALDI-TOF MASS spectra were recorded on a Voyager DE-RP (Applied Biosystems, Foster City, CA, USA) using α-cyano-4-hydroxycinnamic acid as matrix. Analytical HPLC was performed using a C18 reverse-phase column (4.6 × 150 mm; YMC Pack ODS-AM; YMC Co., Ltd, Kyoto, Japan) with a binary solvent system: a linear gradient of 0–100% CH_3CN in 0.1% aqueous TFA over 40 min at a flow rate of 0.9 mL min^{-1} (40 °C), detected at 230 nm. Preparative HPLC was carried out on a C18 reverse-phase column (20 × 250 mm; YMC Pack ODS-AM; YMC Co., Ltd) with a binary solvent system: a linear gradient of CH_3CN in 0.1% aqueous TFA at a flow rate of 5.0 mL min^{-1} (40 °C), detected at 230 nm. Solvents used for HPLC were of HPLC grade.

4.2. Synthesis of *O*-acyl isopeptides of Aβ1–40(WT) and Aβ1–40(E22Δ)

The *O*-acyl isopeptides of Aβ1–40(WT) and Aβ1–40(E22Δ) were synthesized in a similar manner to Ref. 4. Briefly, after protected Aβ27–40-resin (chlorotrityl chloride resin, 0.07-mmol scale) was synthesized by conventional Fmoc-based solid phase peptide synthesis, Boc-Ser-OH (0.18 mmol) was coupled with the *N*,*N*′-diisopropylcarbodiimide (DIC)–*N*-hydroxybenzotriazole (HOBt) (0.18 mmol each) for 2 h in DMF. Fmoc-Gly-OH (1.08 mmol) was coupled to the β-hydroxyl group Boc-Ser[26] using DIC (1.08 mmol)–*N*,*N*-dimethyl-4-aminopyridine (DMAP, 0.02 mmol) in CH_2Cl_2 for 4 h (2×). Subsequent amino acid residues were coupled after removing each Fmoc group using 20% piperidine for 20 min (obtained peptide-resin after the solid phase peptide synthesis: WT: 369 mg; E22Δ: 353 mg). The resulting protected peptide-resin (180 mg each) was treated with TFA–*m*-cresol–thioanisole–H_2O (92.5:2.5:2.5:2.5) for 90 min, concentrated in vacuo, washed with diethyl ether, centrifuged, suspended in water, and lyophilized to give the crude *O*-acyl isopeptide (WT: 75 mg; E22Δ: 83 mg). This peptide (21 mg each) was dissolved in aqueous TFA in the presence of NH_4I (2.0 mmol) and dimethylsulfide (2.0 mmol) and stood for 60 min at 0 °C. After concentration in vacuo, the crude peptide was dissolved in dimethyl sulfoxide (DMSO) and applied to preparative HPLC, and eluted using a 0.1% aqueous TFA–CH_3CN. The desired fractions were collected and immediately lyophilized to afford the peptide as a white amorphous powder. *O*-Acyl isopeptide of Aβ1–40(WT): Yield: 4.7 mg (12.7%); MALDI-MS (TOF): M_{calcd}: 4329.8; $M+H_{found}$: 4330.7; HPLC analysis at 230 nm (injection solvent: DMSO): retention time was 20.4 min, purity was >95% (Fig. S6A). *O*-Acyl isopeptide of Aβ1–40(E22Δ): yield: 5.4 mg (15.8%); MALDI-MS (TOF): M_{calcd}: 4200.7; $M+H_{found}$: 4201.8; HPLC analysis at 230 nm (injection solvent: DMSO): retention time was 20.5 min, purity was >95% (Fig. S6B).

4.3. Conversion of *O*-acyl isopeptides to Aβ1–40(WT) and Aβ1–40(E22Δ) in phosphate buffer (pH 7.4)

The productions of Aβ1–40(WT) (**1**) and Aβ1–40(E22Δ) (**2**) from their corresponding *O*-acyl isopeptides in phosphate buffer (pH 7.4) were performed in a similar manner as described in Ref. 6. Briefly, the *O*-acyl isopeptide in a 0.1% aqueous TFA solution was diluted with an equal volume of phosphate buffer (0.2 M, pH 7.4), and then additional phosphate buffer (0.1 M, pH 7.4) was added to obtain the peptide solution (pH 7.4). The solution was incubated at 37 °C, mixed with an equal volume of hexafluoro-2-propanol (HFIP) at the desired time points (5, 15 and 30 s and 1, 2, 5, 15 and 30 min) to quench the migration reaction, and analyzed by analytical HPLC. MALDI-MS (TOF) for generated **1**: M_{calcd}: 4329.8; $M+H_{found}$: 4330.9; for **2**: M_{calcd}: 4200.7; $M+H_{found}$: 4201.9.

4.4. Sample preparation

The stock solutions of *O*-acyl isopeptides of **1**–**4** as a 0.1% aqueous TFA were prepared in a similar manner as described in Ref. 6. In brief, 0.1% aqueous TFA solutions with *O*-acyl isopeptides were ultra-centrifuged (435,000*g*) at 4 °C for 3 h. The peptide concentration of each solution was estimated from a UV absorption at 280 nm on a BioSpec-1600 (Shimadzu Co., Kyoto, Japan), using a Tyr extinction coefficient of 1490 M^{-1} cm^{-1}. The solutions of peptides were further diluted with aqueous TFA (0.1%) to obtain 220 μM of *O*-acyl isopeptides. Each solution was stored at −80 °C until use. Just before the experiments, the stock solution of *O*-acyl isopeptides were thawed and diluted with an equal volume of phosphate buffer (0.2 M, pH 7.4). Then additional phosphate buffer (0.1 M, pH 7.4) was immediately added to obtain the peptide solution at the desired concentrations.

4.5. Circular dichroism spectrometry

The CD spectroscopy data was obtained in a similar manner to that described in Ref. 6. In brief, buffer solutions containing **1**–**4** (10 μM each peptide) were incubated at 37 °C and applied to the CD spectrometer at the desired time points. CD spectra were measured at 37 °C on a J-720WI (JASCO Corporation, Tokyo, Japan) instrument using a 1.0 mm path length quartz cell. Four scans were averaged for each sample. Averaged blank spectra were subtracted, respectively.

4.6. Western blot with SDS–PAGE

SDS–PAGE was performed in a similar manner to that described in Ref. 8. Incubated sample solutions of **1**–**4** (10 μM each peptide) were mixed with lithium dodecyl sulfate and the mixtures were heated at 70 °C for 10 min. Then the sample was analyzed on Nu-PAGE® Bis–Tris 4–12% gel using MES SDS running Buffer (Invitrogen) under non-reducing conditions. The sample was transferred to polyvinylidene difluoride membrane (Bio-Rad Laboratories Inc., Hercules, CA, USA). The membrane was blocked in 5% skim milk in Tris-buffered saline containing 0.1% Tween 20, incubated with the primary antibody 6E10 (Covance), and then incubated with horseradish peroxidase-conjugated anti-mouse IgG antibody. We developed the membrane using enhanced chemiluminescence (ECL; GE Healthcare).

4.7. Thioflavin-T (ThT) assay

The ThT fluorescence intensity was examined in a similar manner as that described in Ref. 6. In brief, sample solutions of **1**–**4** were incubated at 37 °C (10 μM each peptide) and applied for ThT assay at the desired time points. The aliquot sample (0.15 nmol) was added to 5 μM ThT (Sigma–Aldrich Inc.)-containing glycine buffer (pH 8.5, 1.5 μL). ThT fluorescence at 480 nm was measured at an excitation wavelength of 440 nm on a VersaFluor (Bio-Rad). ThT fluorescence intensity was calculated from a standard fluorescence intensity of a calcein solution (Dojindo Laboratories, Kumamoto, Japan) in phosphate buffered saline (pH 7.4).

4.8. Cytotoxicity assay with PC12 cells

\PC12 cells were cultured and the cytotoxicity was examined in a similar manner to that described in Ref. 8. The cells in HEPES–DMEM containing 5% (v/v) horse serum and 10% (v/v) FBS were seeded at a density of 5000 cells/100 μL/well on a poly-D-lysine-coated 96-well plate (Becton Dickinson Labware) and incubated for 3 days (1 day in case of NGF-differentiated PC12 cells) at 37 °C under 10% CO_2. After the medium was removed, the cells were washed with serum-free HEPES buffered DMEM. Then, the cells were pre-incubated in 100 μL of 25 mM HEPES buffered DMEM (pH 7.4) containing 1% (v/v) horse serum at 37 °C under 10% CO_2 for 1 day. Instead, in the case of NGF-differentiated PC12 cells, the cells were pre-incubated in 100 μL of 25 mM HEPES buffered DMEM (pH 7.4) containing 50 ng mL^{-1} of NGF (serum-free) at 37 °C under 10% CO_2 for 4 days. 10 μL of 0.1% aqueous TFA solution of **1**–**4** was added to the well containing 100 μL cell culture medium (final **1**–**4** concentration: 20 μM each; pH 7.4) and incubated for 48 h at 37 °C under 10% CO_2. A cell count reagent SF containing WST-8 (Nacalai Tesque) was added to each well and the plate was incubated. The colorimetric determination of PC12 cells was made on a Microplate Reader SH-1000 Lab (Corona Electric Co., Ltd, Ibaraki, Japan). The absorption

values at 450 nm (reference: 655 nm) were measured. Values are expressed as mean ± SE (n = 3).

Acknowledgments

This research was supported in part by the 'Academic Frontier' Project for Private Universities: matching fund subsidy from MEXT (Ministry of Education, Culture, Sports, Science and Technology) of the Japanese Government, a Grant-in-Aid for Scientific Research (KAKENHI), Kyoto Pharmaceutical University Fund for the Promotion of Scientific Research, and Takeda Science Foundation. We thank Mr. H. Kawashima for technical assistances. We thank Dr. J.-T. Nguyen for his revision of the manuscript.

Supplementary data

Supplementary data associated with this article can be found, in the online version, at doi:10.1016/j.bmc.2011.04.056.

References and notes

1. Hardy, J.; Selkoe, D. J. *Science* **2002**, *297*, 353.
2. Rahimi, F.; Shanmugam, A.; Bitan, G. *Curr. Alzheimer Res.* **2008**, *5*, 319.
3. Sohma, Y.; Sasaki, M.; Hayashi, Y.; Kimura, T.; Kiso, Y. *Tetrahedron Lett.* **2004**, *45*, 5965.
4. Sohma, Y.; Hayashi, Y.; Kimura, M.; Chiyomori, Y.; Taniguchi, A.; Sasaki, M.; Kimura, T.; Kiso, Y. *J. Pept. Sci.* **2005**, *11*, 441.
5. Kiso, Y.; Taniguchi, A.; Sohma, Y. In *Wiley Encyclopedia of Chemical Biology*; Wiley & Sons: Hoboken, 2009; Vol. 1, p 379.
6. Taniguchi, A.; Sohma, Y.; Hirayama, Y.; Mukai, H.; Kimura, T.; Hayashi, Y.; Matsuzaki, K.; Kiso, Y. *ChemBioChem* **2009**, *10*, 710.
7. Wang, H.; Kakizawa, T.; Taniguchi, A.; Mizuguchi, T.; Kimura, T.; Kiso, Y. *Bioorg. Med. Chem.* **2009**, *17*, 4881.
8. Sohma, Y.; Hirayama, Y.; Taniguchi, A.; Mukai, H.; Kiso, Y. *Bioorg. Med. Chem.* **2011**, *19*, 1729.
9. Santos, S. D.; Chandravarkar, A.; Mandal, B.; Mimna, R.; Murat, K.; Saucède, L.; Tella, P.; Tuchscherer, G.; Mutter, M. *J. Am. Chem. Soc.* **2005**, *127*, 11888.
10. Tuchscherer, G.; Chandravarkar, A.; Camus, M. S.; Bèrard, J.; Murat, K.; Schmid, A.; Mimna, R.; Lashuel, H. A.; Mutter, M. *Biopolymers* **2007**, *88*, 239.
11. Balducci, C.; Beeg, M.; Stravalaci, M.; Bastone, A.; Sclip, A.; Biasini, E.; Tapella, L.; Colombo, L.; Manzoni, C.; Borsello, T.; Chiesa, R.; Gobbi, M.; Salmona, M.; Forloni, G. *Proc. Natl. Acad. Sci. U.S.A.* **2010**, *107*, 2295.
12. Bozso, Z.; Penke, B.; Simon, D.; Laczkó, I.; Juhász, G.; Szegedi, V.; Kasza, A.; Soós, K.; Hetényi, A.; Wéber, E.; Tóháti, H.; Csete, M.; Zarándi, M.; Fülöp, L. *Peptides* **2010**, *31*, 248.
13. Taylor, M.; Moore, S.; Mayes, J.; Parkin, E.; Beeg, M.; Canovi, M.; Gobbi, M.; Mann, D. M. A.; Allsop, D. *Biochemistry* **2010**, *49*, 3261.
14. Beeg, M.; Stravalaci, M.; Bastone, A.; Salmona, M.; Gobbi, M. *Anal. Biochem.* **2011**, *411*, 297.
15. Sohma, Y.; Sasaki, M.; Hayashi, Y.; Kimura, T.; Kiso, Y. *Chem. Commun.* **2004**, *111*, 124.
16. Carpino, L. A.; Krause, E.; Sferdean, C. D.; Schuemann, M.; Fabian, H.; Bienert, M.; Beyermann, M. *Tetrahedron Lett.* **2004**, *45*, 7519.
17. Mutter, M.; Chandravarkar, A.; Boyat, C.; Lopez, J.; Santos, S. D.; Mandal, B.; Mimna, R.; Murat, K.; Patiny, L.; Saucède, L.; Tuchscherer, G. *Angew. Chem., Int. Ed.* **2004**, *43*, 4172.
18. Hentschel, J.; Krause, E.; Börner, H. G. *J. Am. Chem. Soc.* **2006**, *128*, 7722.
19. Shigenaga, A.; Tsuji, D.; Nishioka, N.; Tsuda, S.; Itoh, K.; Otaka, A. *ChemBioChem* **2007**, *8*, 1929.
20. Natalia, N.; Valerie, G.; Aviv, C.; Saviana, D.; Hilal, A. L.; Ashraf, B. *Org. Lett.* **2008**, *10*, 5243.
21. Vila-Perello, M.; Hori, Y.; Ribo, M.; Muir, T. W. *Angew. Chem., Int. Ed.* **2008**, *47*, 7764.
22. Lécaillon, J.; Gilles, P.; Subra, G.; Martinez, J.; Amblard, M. *Tetrahedron Lett.* **2008**, *49*, 4674.
23. Boussert, S.; Diez-Perez, I.; Kogan, M. J.; de Oliveira, E.; Giralt, E. *ACS Nano* **2009**, *3*, 3091.
24. Cao, P.; Raleigh, D. P. *J. Am. Chem. Soc.* **2010**, *132*, 4052.
25. Tomiyama, T.; Nagata, T.; Shimada, H.; Teraoka, R.; Fukushima, A.; Kanemitsu, H.; Takuma, H.; Kuwano, R.; Imagawa, M.; Ataka, S.; Wada, Y.; Yoshioka, E.; Nishizaki, T.; Watanabe, Y.; Mori, H. *Ann. Neurol.* **2008**, *63*, 377.
26. Takuma, H.; Teraoka, R.; Mori, H.; Tomiyama, T. *Neuroreport* **2008**, *19*, 615.
27. Tomiyama, T.; Matsuyama, S.; Iso, H.; Umeda, T.; Takuma, H.; Ohnishi, K.; Ishibashi, K.; Teraoka, R.; Sakama, N.; Yamashita, T.; Nishitsuji, K.; Ito, K.; Shimada, H.; Lambert, M. P.; Klein, W. L.; Mori, H. *J. Neurosci.* **2010**, *30*, 4845.
28. Walsh, D. M.; Selkoe, D. J. *J. Neurochem.* **2007**, *101*, 1172.
29. Suzuki, T.; Murakami, K.; Izuo, N.; Kume, T.; Akaike, A.; Nagata, T.; Nishizaki, T.; Tomiyama, T.; Takuma, H.; Mori, H.; Irie, K. *Int. J. Alzheimer's Disease* Vol. 2011, Article ID 431320, 8 pages, 2011. doi: 10.4061/2011/431320.
30. Cloe, A. L.; Orgel, J. P. R. O.; Sachleben, J. R.; Tycko, R.; Meredith, S. C. *Biochemistry* **2011**, *50*, 2026.
31. While this paper was being prepared for publication a property of Aβ(E22Δ) prone to form β-sheet structure was reported in Refs. 29 and 30, respectively.
32. Bitan, G.; Kirkitadze, M. D.; Lomakin, A.; Vollers, S. S.; Benedek, G. B.; Teplow, D. B. *Proc. Natl. Acad. Sci. U.S.A.* **2003**, *100*, 330.
33. Murakami, K.; Irie, K.; Morimoto, A.; Ohigashi, H.; Shindo, M.; Nagao, M.; Shimizu, T.; Shirasawa, T. *J. Biol. Chem.* **2003**, *278*, 46179.
34. Ono, K.; Condron, M. M.; Teplow, D. B. *J. Biol. Chem.* **2010**, *285*, 23186.